TESLA Report 2003-23

NEAR-WALL WAKEFIELDS FOR OPTIMIZED GEOMETRY OF TTF 2 COLLIMATOR

I. Zagorodnov, T. Weiland

Technische Universität Darmstadt
Institut für Theorie Elektromagnetischer Felder (TEMF)
Schloßgartenstraße 8, D 64289 Darmstadt, Germany

M.Dohlus, M.Körfer

Deutsches Elektronen-Synchrotron (DESY)
Gruppe Beschleunigerphysik
Notkestraße 85, D 22607 Hamburg, Germany

(Dated: June 25, 2003)

Abstract

Wakefields excited in the small aperture collimators may damage the beam. As pointed out by K. Bane and P. Morton the wakefields can be reduced considerably by tapering the steps and using the "step+taper" collimator geometry. The optimisation of this kind of geometry for TTF 2 collimators with different apertures is carried out in the paper. For the optimal geometries the non-linear near-wall wakefields are calculated. The numerical results are confirmed by comparison with analytical estimations for the fully tapered collimator in inductive regime.

1 INTRODUCTION

Transverse wakefields excited in the collimators may damage the beam due to the small aperture of the scraper. As pointed out in [1] a possible way to relax the wakefields is tapering the steps and using “step+taper” collimator geometry. The optimisation of this kind of geometry for TTF 2 collimators with different apertures is carried out in the paper.

The TTF2 operation requires very short bunches with RMS $s = 50mm$ that forces us to use the dense mesh and the long integration path. That is why up to date only a circular collimators can be studied and the indirect method for calculation of wake potential [2] has to be applied.

The considered collimator is axially symmetric, therefore the problem can be reduced to a set of independent two dimensional problems for the azimuthal modes.

The aperture of the collimator is small and a good estimation of the near-wall wakefields can be important. Unlike the near-axis case to estimate the near-wall wakefields not only monopole and dipole modes but also higher order modes need to be calculated.

The conventional codes like MAFIA [3] and TBCI [4] have difficulties in solving the described problem and a new code ECHO [5] is used for numerical experiments.

In the paper we calculate near-wall wakefields for the optimized collimator geometry and check the results by comparing the calculated near-wall wakes with the analytical estimation of Yokoya [6] for tapered collimator.

2 MODES NUMBER ESTIMATION

This paper deals with circular collimators whose geometries are outlined in the Fig.1,6.

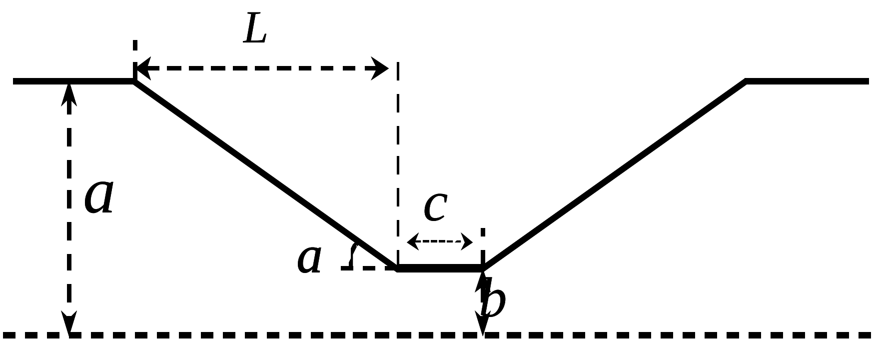

Fig.1. Geometry of the collimator

The longitudinal and transversal wake functions can be written in the form [7]

$$w_{\parallel}(s, r_e, j_e, r_o, j_o) = \sum_{n=0}^{\infty} w_{\parallel}^m(s) r_e^{\,m} r_o^{\,m} \cos m(j_0 - j_e),$$

$$\begin{pmatrix} w_r \\ w_j \end{pmatrix}(s, r_e, j_e, r_o, j_o) = \sum_{n=1}^{\infty} m w_{\perp}^m(s) r_e^{\,m-1} r_o^{\,m} \begin{pmatrix} -\cos m(j_0 - j_e) \\ \sin m(j_0 - j_e) \end{pmatrix},$$

where (r_e, j_e), (r_o, j_o) are the coordinates of the excitation and observation electrons and the functions $w_{\parallel}^m(s)$, $w_{\parallel}^m(s)$ are related by Panofsky-Wenzel theorem

$$w_{\perp}^m(s) = \int_0^s w_{\parallel}^m(z) dz .$$

Because of the explicit dependency of the wake functions on the angles and the radii, only the situation $r_e = r_o = r_b$, $j_e = j_o = 0$ will be discussed.

To get the total wakefield effect we need to sum over all multipole contributions. Usually bunches remain near to the axis and the longitudinal wakefield effect is dominated by the monopole mode (m=0) whereas the transverse one is dominated by the dipole mode (m=1). However, if we want to consider near-wall wake fields we have to calculate higher order modes too. The number of the required modes depends on the closeness d of the bunch moving at the radius r to the boundary $f(z)$:

$$d(r) = \frac{r}{b} \ , \ b = \min\ f(z)\, , r \le b \, .$$

To study the question how many modes are required for the desired accuracy we consider first the analytical estimation of K. Yokoya for wakes of small-angle collimators and latter in this section we check the result by numerical calculations for a specific problem.

As shown in [6], for small taper angles $r = \tan(a) b / s \ll 1$ (s is a width of Gaussian bunch) the collimator is in the *inductive* regime and the impedance estimations read

$$Z_{\parallel}^0 = \Theta \frac{iw}{c^2} \int_{-\infty}^{\infty} (f')^2\, dz \ , \ Z_{\parallel}^m = \frac{w}{mc} Z_{\perp}^m \, , \tag{1}$$

$$Z_{\perp}^m = \Theta \frac{4im}{c(m+1)} \int_{-\infty}^{\infty} \left(\frac{f'}{f^m} \right)^2 dz \, , \tag{2}$$

where $\Theta = Z_0 c / 4p$, and Z_0 is the free space impedance.

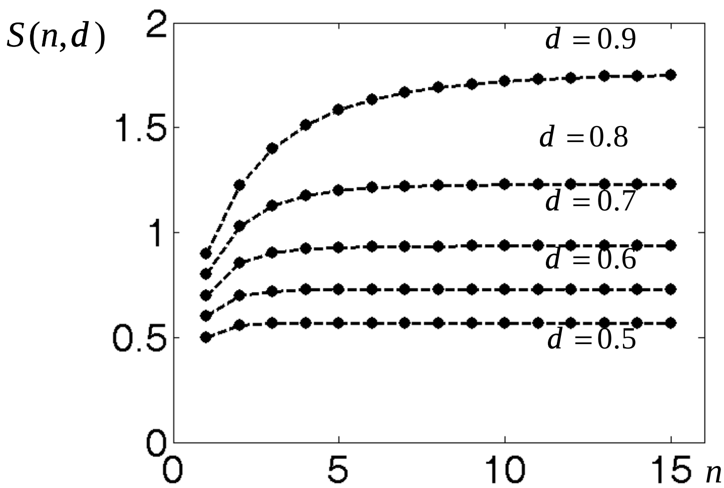

Fig2. Dependency of the sum $S(n,d)$ on number of modes n for different offsets d .

As follows from expressions (1), (2), the transversal impedance for the charges moving at the radius r can be written in the form

$$Z_{\perp}(r) = \sum_{m=1}^{\infty} Z_{\perp}^m r^{2m-1} \ , \ Z_{\perp}^m r^{2m-1} = \Theta \frac{8i}{c} \tan(a) \frac{m}{(m+1)(2m-1)} \left(d(r)^{2m-1} - \left(\frac{r}{a} \right)^{2m-1} \right) . \tag{3}$$

The last term $(r/a)^{2m-1}$ can be neglected and relation (3) is reduced to

$$Z_{\perp}(r) \cong \Theta \frac{4i}{c} \tan(a)\, 2 \sum_{m=1}^{\infty} \frac{m d(r)^{2m-1}}{(m+1)(2m-1)} \, . \tag{4}$$

The addends of sum (4) for $d = 1$ behave like $O(m^{-1})$ and the sum diverges. Consequently we consider only the case $d<1$ when the sum converges with a rate depending on d. Note that due to (1) the longitudinal impedance has a modal sum with $O(m^{-2})$ behavior which converges fast even on the boundary $d=1$.

In Fig.2 the dependency of the sum

$$S(n,d)=2\sum_{m=1}^{n}\frac{md(r)^{2m-1}}{(m+1)(2m-1)} \tag{5}$$

is shown and in Table 1 the relative error

$$\Delta S(n,d)=\frac{|S(n,d)-S(\infty,d)|}{S(\infty,d)}\cong\frac{|S(n,d)-S(100,d)|}{S(100,d)} \tag{6}$$

is presented. We see that n=7 addends of sum (5) present the result with an accuracy of ~5% up to offset $d=0.9$. Hence, in the numerical calculations discussed below we are looking only for the first 8 modes (the monopole mode $m=0$ should not be forgotten). Note that the dipole mode $n=m=1$ alone gives only 50% of the kick for the near-wall charges with an offset $d=0.9$.

d	n			
	1	2	3	7
0.5	12	2	0.4	0.001
0.6	18	4.5	1.2	0.01
0.7	25	8.8	3.5	0.1
0.8	35	16	8.4	0.8
0.9	49	30	20	5.3

Table 1. Relative error $\Delta S(n,d)$ in % for different number of modes n and offsets d

As a next step we compare analytical estimation (3) with numerical results obtained by the code ECHO [5]. The fully tapered test collimator has the parameters: $a=17mm$, $b=2mm$, $c=100mm$, $L=200mm$. We calculate the kick factor ($j_e=j_o$, $r_e=r_o=r$)

$$L_{\perp}=\frac{1}{Q}\int_{-\infty}^{\infty}W_{\perp}(s)q(s)ds=\frac{1}{Q^2}\int_{-\infty}^{\infty}\int_{-\infty}^{s}w_{\perp}(s-s')q(s')q(s)ds'ds\ ,$$

$$w_{\perp}(s,r)=\sum_{m=1}^{\infty}mw_{\perp}^{m}(s)r^{2m-1}$$

for a Gaussian bunch $q(s)$ with RMS length $s=500mm$. In this case $r=\tan(a)b/s=0.3$ and the collimator is in the inductive regime that allows to apply estimation (2) for transversal impedance.

Fig.3 shows the dependency of the sum

$$L_{\perp}(n,d)=\sum_{m=1}^{n}L_{\perp}^{m}(db)^{2m-1} \tag{7}$$

on the number of modes, where $L_{\perp}^{m}$ is a modal kick factor. The dashed lines show the analytical estimation and the solid lines show the numerical results. The calculations were done with a mesh resolution of 10 mesh steps on s ($s/h=10$, h is a mesh step), resulting in an accuracy better than 1% (checked by thickening of the mesh).

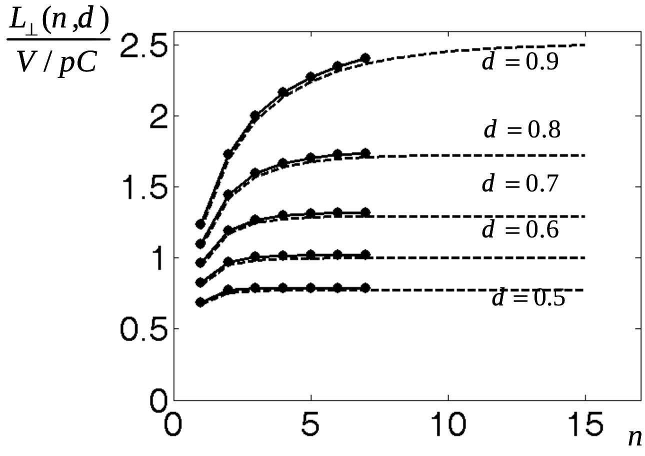

Fig 3. Dependency of the kick factor sum $L_\perp(n,d)$ on the number of modes n for different offsets d for a fully tapered test collimator and a Gaussian bunch with RMS length $s = 500mm$

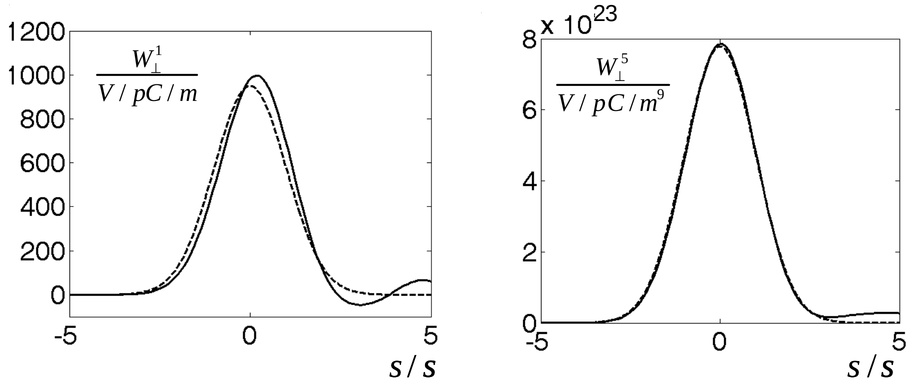

Fig 4. The transverse modal wake potentials of the test geometry for modes $m=1$ (left) and $m=5$ (right). The Gaussian bunch has the RMS length $s = 500mm$.

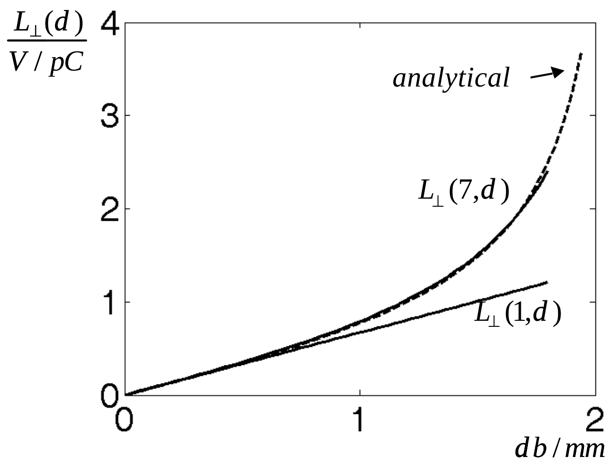

Fig 5. Dependence of the transversal kick $L_\perp$ on an offset d .

Fig. 4 shows the transverse modal wake potential for modes $m=1$ (left) and $m=5$ (right). The solid lines correspond to the numerical results with $s/h=10$ and the dashes display the analytical estimations (2).

Fig. 5 shows the dependency of the transverse kick on the offset d from the axis. We compare numerical (solid lines) and analytical (dashed line) results for the case when 8 modes ($m = 0,1,2,...,7$) are taken into account. The numerical results are shown up to $d = 0.9$. The analytical curve is calculated with 15 modes up to the closeness $d = 0.95$.

In the discussed test problem a very good coincidence of the numerical and analytical results is obtained. On the other hand the results in Fig.3 looks very like the ones shown in Fig.1 and the estimations presented in Table 1 hold for both cases.

Before estimating of the near-wall wake fields for a real set of parameters we will first concentrate on the optimization of the "taper+step" geometry with regard to the near-axis wakes (monopole and dipole modes).

3 GEOMETRY OPTIMIZATION

As pointed out in [1] a possible way to relax the wakefields is tapering that actually reduces considerably the wakes of the collimator. However, in order to obtain a significant effect the collimator has to be too long. As an alternative solution we consider the "step+taper" geometry of a collimator with a fixed length of $50cm$ as shown in Fig.5. The effectiveness of such kind of geometry was proven in [1]. The set of parameters shown in Fig. 5 corresponds to the TESLA TTF2 collimator at DESY [8]. The calculations are carried out for very short Gaussian bunch with $s = 0.05mm$.

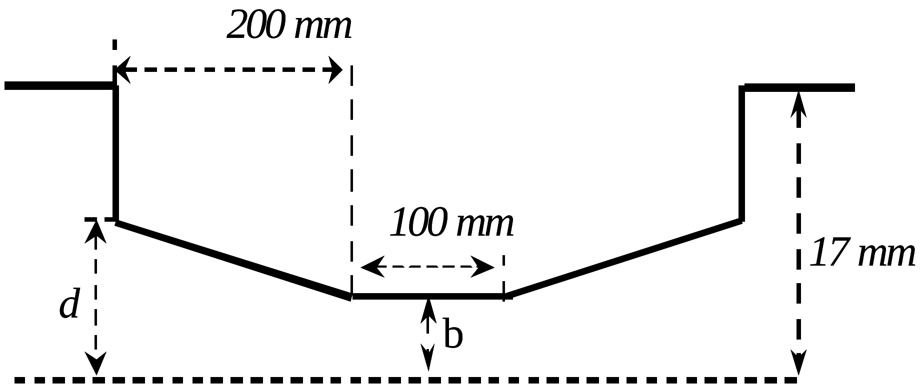

Fig 6. Geometry of the "step+taper" collimator

Three different apertures b of the collimator are considered: $b = 2mm$, $3mm$ and $6mm$. The parameter d changes from b (step collimator) to $a = 17mm$ (fully tapered collimator). We consider only near-axis wakes and consequently only monopole and dipole modes are calculated. As optimization parameters we have chosen the loss factor

$$L_{\parallel} \cong \left\langle W_{\parallel}^{0} \right\rangle = \frac{1}{Q}\int_{-\infty}^{\infty} W_{\parallel}^{0}(s) q(s) ds = \frac{1}{Q^2}\int_{-\infty}^{\infty}\int_{-\infty}^{s} w_{\parallel}^{0}(s-s') q(s') q(s) ds' ds,$$

the RMS energy spread

$$\left\langle \left(\Delta W_{\parallel}^{0}\right)^2 \right\rangle^{1/2} = \left[\frac{1}{Q}\int_{-\infty}^{\infty}\left(\left\langle W_{\parallel}^{0}\right\rangle - W_{\parallel}^{0}(s)\right)^2 q(s) ds\right]^{1/2},$$

the kick factor

$$L_{\perp} \cong \left\langle W_{\perp}^{1} \right\rangle = \frac{1}{Q}\int_{-\infty}^{\infty} W_{\perp}^{1}(s) q(s) ds = \frac{1}{Q^2}\int_{-\infty}^{\infty}\int_{-\infty}^{s} w_{\perp}^{1}(s-s') q(s') q(s) ds' ds$$

and the RMS kick spread

$$\left\langle \left(\Delta W_\perp^1\right)^2 \right\rangle^{1/2} = \left[\frac{1}{Q}\int_{-\infty}^{\infty}\left(\left\langle W_\perp^1\right\rangle - W_\perp^1(s)\right)^2 q(s)ds\right]^{1/2}.$$

For the case $b = 2mm$ Fig. 7 shows dependence of the loss factor, energy spread, kick factor, kick spread on the parameter d. The depicted functions have minimums and the value $d = 4.5mm$ can be taken as the optimum.

Fig. 8-9 presents likewise the results for the aperture $b = 3mm$ and $6mm$.

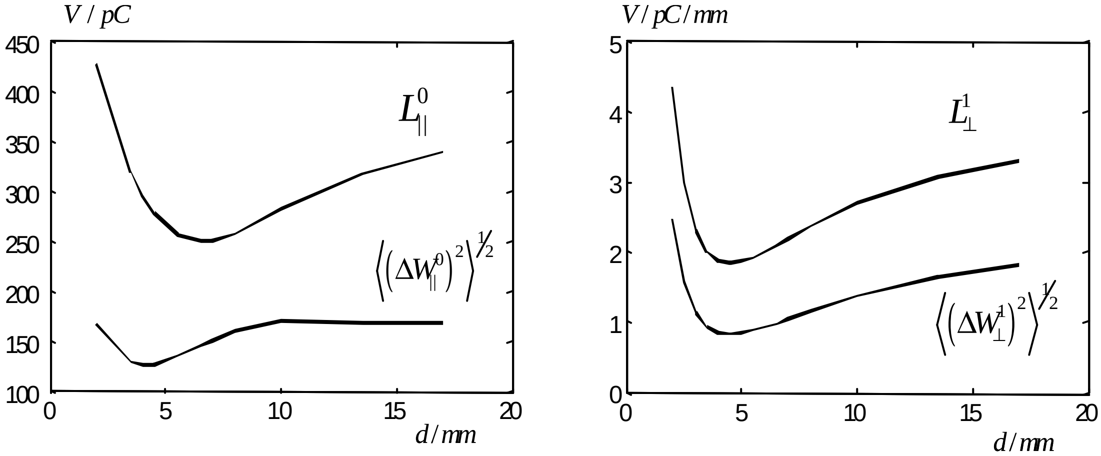

Fig 7. The integral parameters for aperture $b = 2mm$.

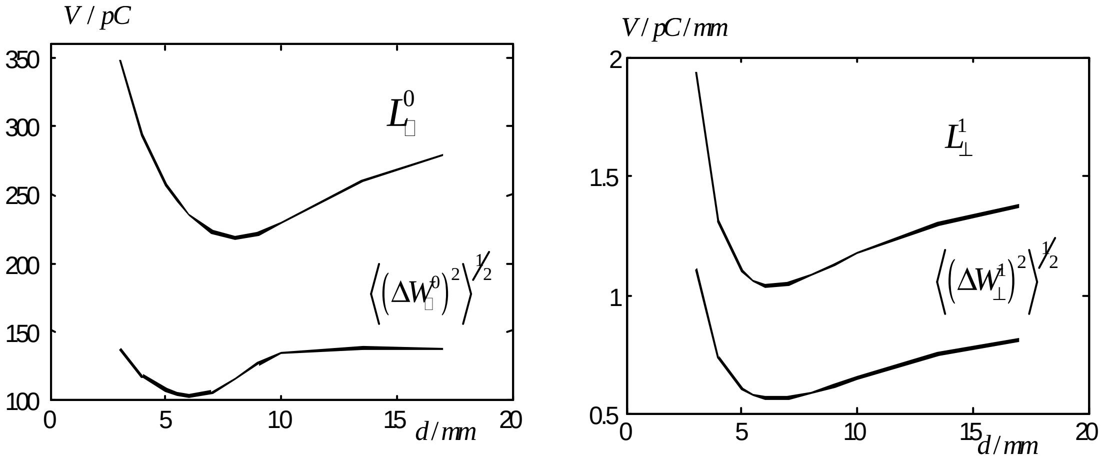

Fig 8. The integral parameters for aperture $b = 3mm$.

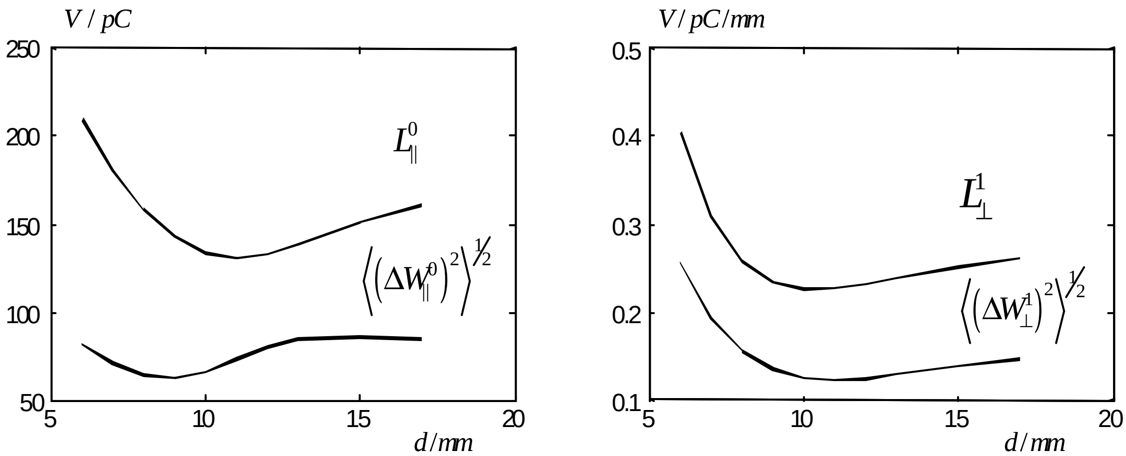

Fig 9. The integral parameters for aperture $b = 6mm$.

We do not introduce a goal function for the optimization process as the four optimized integral parameters have their minimums approximately at the same point for each of the considered cases. Table 2 summarizes the optimal sets of parameters.

b, mm	2	3	6
d, mm	4.5	5.5	10

Table 2. Optimal sets of parameters for the "step+taper" collimator.

Finally, in Fig. 10 the longitudinal and transverse wake potentials are shown for the aperture $b = 2mm$ and three different cases: $d = 2mm$ (step collimator), $d = 17mm$ (fully tapered collimator) and $d = 4.5mm$ (optimal "step+taper" geometry, solid lines).

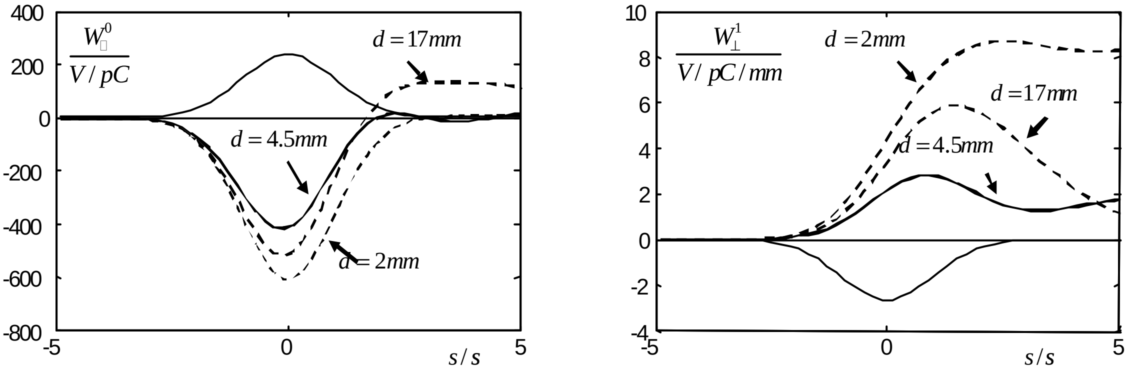

Fig 10. The integral parameters for aperture $b = 2mm$.
The Gaussian bunch has the RMS length $s = 50mm$.

As can be seen the "step+taper" geometry of the collimator allows indeed reduce the wakefields effects considerably.

The near-wall wakefields are considered in the next section only for the geometry with the smallest collimator aperture.

4 NEAR-WALL WAKES

Because the aperture of the collimator is small the near-wall wake fields can play considerable role in single bunch dynamics. In this section the near-wall wake fields for the optimized "step+taper" geometry with the smallest aperture $b = 2\ mm$ are considered. The parameter d is equal to $4.5\ mm$. The mode integral parameters are calculated for the first 8 modes, m=0,.1,…,7. The bunch has the RMS length $s = 50mm$, threfore analytical estimations (1), (2) are not valid.

Fig.11 shows the transverse wake potentials for the modes $m = 1$ (left) and $m = 7$ (right). The potentials are calculated with different mesh resolutions :$s\ /h = 5$ (dashed lines), $s\ /h = 10$ (solid lines) , where h is a mesh step. On the left figure the curves coincide and on the right picture the difference increases with the mode number. Hence the higher order modes demand a better mesh resolution and all modes were estimated with a resolution $s\ /h = 10$.

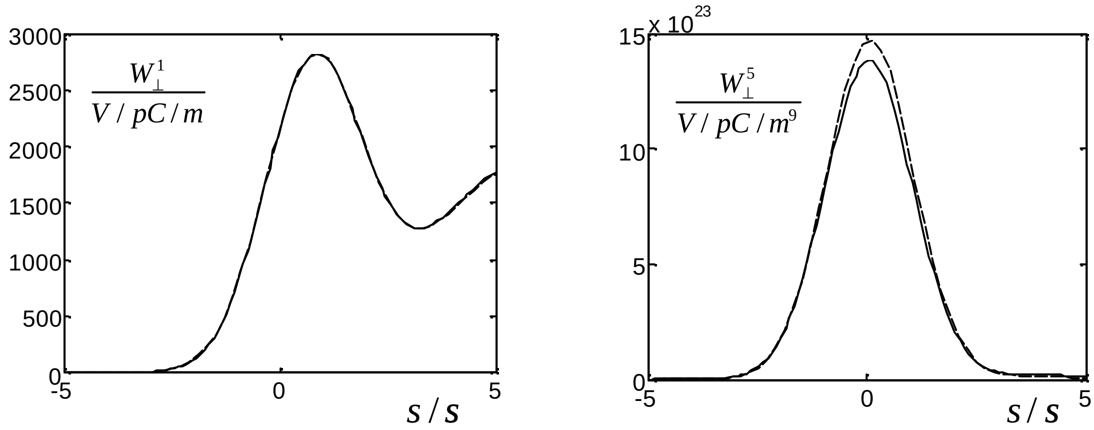

Fig 11. The transverse modal wake potential of TTF2 colimator for modes $m=1$ (left) and $m=5$ (right). The Gaussian bunch has the RMS length $s = 50mm$.

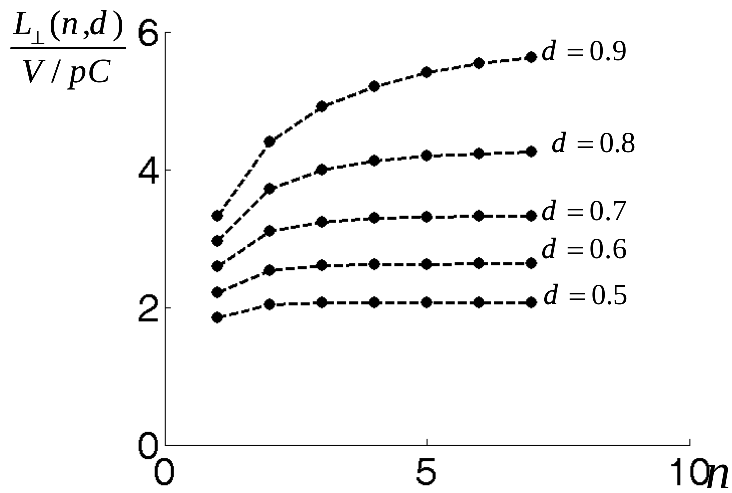

Fig 12. Dependency of the kick factor sum $L_\perp(n,d)$ on the number of modes n for different offsets d and the optimal "step+taper" collimator. The Gaussian bunch has RMS length $s = 50mm$

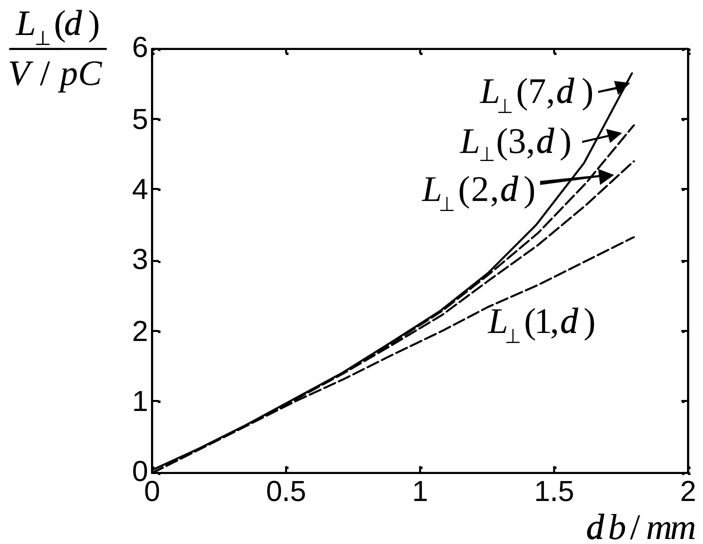

Fig 13. Dependency of the transversal kick $L_\perp$ on the offset d for the optimal "step+taper" collimator and a Gaussian bunch with RMS length $s = 50mm$.

Fig.12 shows the dependency of the kick factor sum (7) on the number of modes as obtained from the numerical calculations. The results are qualitatively similar to the ones presented in Fig.3, therefore we are quite sure that the error estimations given in the Table 1 hold and 8 modes are quite enough to obtain the kick factor for an offset $d = 0.9$ with an accuracy of $\sim 5\%$.

Fig. 13 shows the dependency of the transverse kick on the offset d from the axis. Seven modes $(m = 1,2,...,7)$ are taken into account. The numerical results are shown up to $d = 0.9$ and looks very like the ones presented in Fig.5. As noted in section 2, the sum addends behave like $O(m^{-1})$ and it diverges on the boundary $d = 1$. The effect of non-linear higher order addends of the sum has to be taken into account for bunch offsets $d > 1/4$. The dipole mode alone presents 59% of the kick factor for $d = 0.9$.

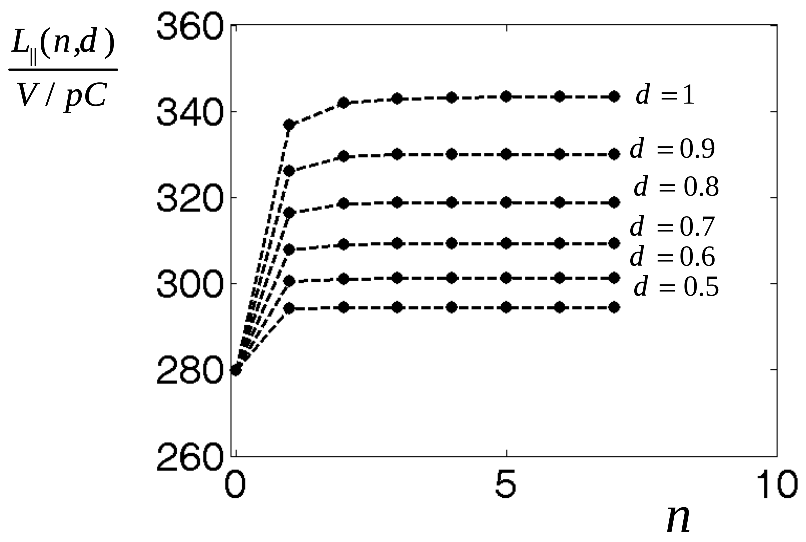

Fig 14. Dependency of the loss factor sum $L_{||}(n,d)$ on the number of modes n for different offsets d.

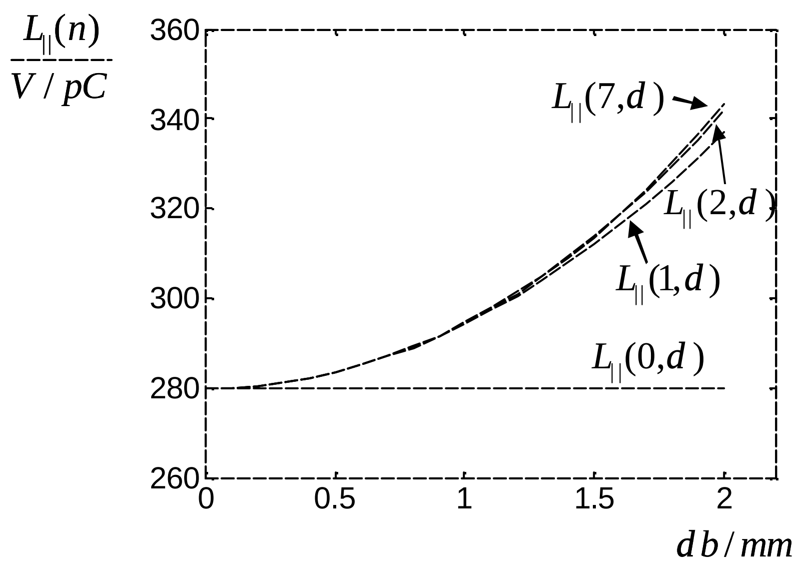

Fig 15. Dependency of the loss factor $L_{||}$ on the offset d.

Fig.14 shows the dependency of the loss factor sum

$$L_{||}(n,d) = \sum_{m=0}^{n} L_{||}^{m} (db)^{2m}$$

on the number of modes, where $L_{||}^{m}$ is a modal loss factor. As noted in section 2, the sum addends behave like $O(m^{-2})$ and it converges fast even on the boundary $d = 1$. The effect of the non-linear higher order addends of the sum is small and already monopole and dipole modes give the estimation with an accuracy of ~2%. The monopole mode alone presents 82% of the loss factor for $d = 1$.

Fig. 15 shows the dependency of the loss factor on the offset d from the axis. Eight modes $(m = 0,2,...,7)$ are taken into account. The numerical results are shown up to the boundary $d = 1$.

CONCLUSION

The short-range geometric wakefields in rotationally symmetric collimators are studied. The geometry of the collimator is optimized for a fixed length. For this optimal geometry the near-wall wakefields are calculated. The accuracy of the numerical estimations is confirmed by considering the test problem of a fully tapered collimator where the analytical estimations are known.

As the numerical and analytical estimations show, the impact of higher order modes on the loss factor is small (less then 20%) relatively to the monopole mode result up to the aperture wall of the collimator.

In contrary the dipole mode alone gives only about 50% of the kick factor when the bunch offset is equal to 0.9 of the collimator aperture radius. The impact of the higher order modes is considerable and has to be taken into account.

According to the applied wakefield model the analytical and numerical estimations show a fast unbounded growth of the kick factor in the near-wall region.

ACKNOWLEDGEMENT

Helpful discussions with K.Bane and R.Brinkmann are acknowledged.

REFERENCES

[1] Bane K.F.L., Morton P.L., *Deflection by the Image Current and Charges of a Beam Scraper*, LINAC 1986, SLAC-PUB-3983

[2] Napoly O, Chin Y, Zotter B., *A Generalized Method for Calculating Wake Potentials*, Num. Instrum. Meth. 1993; **344**:255.

[3] Weiland T., *Time Domain Electromagnetic Field Computation with Finite Difference Methods*, Int. J. Numer. Model., 1996; **9**:295.

[4] Chin Y.H., *User's Guide for ABCI Version 8.7*, CERN-SL-94-02-AP.

[5] Zagorodnov I., Weiland T., *Calculation of Transversal Wake Potential for Short Bunches*, ICAP 2002 (to appear).

[6] Yokoya K., *Impedance of Slowly Tapered Structures*, Tech. Rep. SL/90-88 (AP), CERN, 1990.

[7] Weiland T., Wanzenberg R., *Wake Fields and Impedances*, CCAS-CAT-CERN Accelerator School, Vol. 1, 1993, , pp. 140-180.

[8] Körfer M., *Layout and Functionality of Collimator System*, TESLA Coll. Meeting, Salzau, 21.01.2003.